ELSEVIER

Biochimica et Biophysica Acta 1514 (2001) 33–50

BIOCHIMICA ET BIOPHYSICA ACTA
BBA

www.bba-direct.com

Probing of the substrate binding domain of lactose permease by a proton pulse

E. Nachliel, M. Gutman *

Laser Laboratory for Fast Reaction in Biology, Department of Biochemistry, Tel Aviv University, Tel Aviv, Israel

Received 1 March 2001; received in revised form 28 May 2001; accepted 29 May 2001

Abstract

The lactose permease of *Escherichia coli* coupled proton transfer across the bacterial inner membrane with the uptake of β-galactosides. In the present study we have used the cysteine-less C148 mutant that was selectively labeled by fluorescein maleimide on the C148 residue, which is an active component of the substrate transporting cavity. Measurements of the protonation dynamics of the bound pH indicator in the time resolved domain allowed us to probe the binding site by a free diffusing proton. The measured signal was reconstructed by numeric integration of differential rate equations that comply with the detailed balance principle and account for all proton transfer reactions taking place in the reaction mixture. This analysis yields the rate constants and p*K* values of all residues participating in the fast proton transfer reaction between the bulk and the protein's surface, revealing the exposed residues that react with free protons in a diffusion controlled reaction and how they transfer protons among themselves. The magnitudes of these rate constants were finally evaluated by comparison with the rate predicted by the Debye–Smoluchowski equation. The analysis of the kinetic and p*K* values indicated that the protein–fluorescein adduct assumes two conformation states. One is dominant above pH 7.4, while the other exists only below 7.1. In the high pH range, the enzyme assumes a constrained configuration and the rate constant of the reaction of a free diffusing proton with the bound dye is 10 times slower than a diffusion controlled reaction. In this state, the carboxylate moiety of residue E126 is in close proximity to the dye and exchanges a proton with it at a very fast rate. Below pH 7.1, the substrate binding domain is in a relaxed configuration and freely accessed by bulk protons, and the rate of proton exchange between the dye and E126 is 100 000 times slower. The relevance of these observations to the catalytic cycle is discussed.

Keywords: Lactose permease; Proton pulse; Intra-protein proton transfer; Diffusion controlled reaction

1. Introduction

The lactose permease (lac permease) of *Escherichia coli* is a membrane protein that utilizes the proton's electrochemical gradient ($\Delta\mu H^+$) for accumulation of β-galactosides. The protein was solubilized, purified to homogeneity, reconstituted in lipoprotein vesicles and shown to be the only component needed to drive the transport of galactosides (for a comprehensive review, see [1,2]). Until now, the enzyme has not been crystallized and its proposed structure is based on numerous mutations coupled with chemical modifications and physical measurements. These studies indicate that it has a structure of 12 cross-membranal α helices interconnected by hydrophilic loops [3–6].

Abbreviations: Lac permease, lactose permease; pyranine or ϕOH, 8-hydroxypyrene 1,3,6-trisulfonate; flu, fluorescein

* Corresponding author. Fax: +972-3-640-6834.
E-mail address: me@hemi.tau.ac.il (M. Gutman).

0005-2736/01/$ – see front matter
PII: S0005-2736(01)00361-3

Extensive mutations and evaluation of their catalytic activity indicated that out of the 417 amino acids of the enzyme, only six polar residues, located in the cross-membranal section of the enzyme (E126, R144, E269, R302, H322 and E325), are essential for the catalytic activity [2]. The catalytic cycle of lac permease is associated with conformation transition [7,8]. In these transitions some non-polar moieties are essential components [9].

The catalytic function of lac permease is the combination of two processes [2]. One is the mechanism that converts the $\Delta\mu H^+$ into a substrate driving force by imposing vectoriality on the binding and release of the galactoside. The other process prevents a proton slip during the catalytic cycle; otherwise the enzyme would function as an inherent uncoupler that dissipates the $\Delta\mu H^+$. The large size of the transported substrate, and the strict requirement to maintain a proton leak-proof seal, imply that the protein must undergo extensive conformation transformation [6,10]. Considering that the transported substrate carries no net charge, a model based on direct electrostatic interactions between the enzyme and the substrate cannot account for the proton-galactose co-transport. Accordingly, the substrate transport is probably mediated by timed conformational changes of the protein, which are coupled with replacement of protein–substrate interactions by solvent–substrate stabilization.

In the present study, we monitored the accessibility of the substrate binding domain to the bulk by labeling it with a covalently bound pH indicator (fluorescein maleimide) and monitored the rate of its reaction with protons released in the bulk. The site for labeling was the native cysteine residue (C148) which stabilizes the substrate in the conducting cleft and blocking it by a maleimide derivative inhibits the flux through the enzyme [7,11–14]. The lac permease has a substrate binding site that can accommodate a hydrophilic moiety as large as a disaccharide while maintaining a tight seal conformation that does not allow a proton to leak through the protein. Thus, by probing the proton accessibility into the protein we gain a quantitative parameter for characterizing the inner cavities, which are comparable in depth with the penetration of the native substrate. The usage of an indicator with a molecular weight comparable to that of the substrate (427 and 342 respectively), which is attached to the same residue (C148) that was implicated in the binding of the native substrate, offers the opportunity to probe the inner space of the enzyme under conditions that mimic the state of the enzyme when loaded with the substrate. Indeed, the fluorescein and the lactose are not identical in hydrophobicity, charge and geometry; however, this dye offers the best opportunity to analyze, for the first time, the dynamics of proton transfer between the amino acid's side chains with a reporter group located in the substrate binding site. Thus, even though the binding of a residue that differs from the substrate could have modulated the probed space, the measurements provide novel information about the interaction between moieties within the substrate binding site.

The selection of a pH indicator as a reporter group offers the possibility to probe the environment of the dye by free diffusing proton, particles that drive the substrate flux through the enzyme and are the best gauge particles for probing an environment. The solvated proton is the most studied ion in solution and its equilibration and kinetics are well recognized [15–19]. The rate constant of protonation of a residue by a free diffusing proton is given by the Debye–Smoluchowski equation. For a well-exposed site, the rate constant is $1–2\times10^{10}$ M^{-1} s^{-1} [20]. A slower rate constant implies that the site is located in a hydrophobic environment or that an intensive, positive potential repels the proton. The very same parameters, hydrophobic environment, or a nearby electric charge also affect the pK value of a residue. Thus, the chemico-physical properties of the site can be deduced by combining kinetic and thermodynamic information.

The measuring system in the present study is based on the laser induced proton pulse technology [21–28] where the labeled enzyme is dissolved in a dilute solution of pyranine (8-hydroxypyrene 1,3,6-trisulfonate (ϕOH)) and subjected to a train of short laser pulses. Each pulse excites the pyranine to its first electronic singlet state, lowering its pK from 8.4 (in the ground state at $I=0$) to p$K^*=1.4$, and the hydroxyl proton dissociates before the molecule relaxes to its ground state [29]. Some 10 ns after the pulse, the excited pyranine relaxes to the ground state and the system is poised in a temporary state of disequilibrium where both products (ϕO^- and free protons)

are above their pre-pulse level. The released protons react in a diffusion controlled reaction with all available proton binding sites, and the dynamics of the reaction are followed at 458 and 496 nm, where the pyranine anion and the fluorescein are selectively measured. The dynamics of the chromophores are coupled with the state of protonation of all proton binding sites. The recorded signals are subjected to a kinetic analysis that accounts for the manifold reaction pathways through which the perturbation can relax [31,30].

The analysis reveals that the lac permease fluorescein adduct excites in two conformation states, which are controlled by the pre-pulse pH. In the low pH range (pH $\leq$7.1), the accessibility of the proton to the substrate binding site is of a diffusion controlled reaction, while the interaction of the dye with the nearby carboxylate of E126 is poor. In the high pH regime (pH $\geq$7.4), the proton accessibility is reduced while the carboxylate of E126 and the dye exchange protons at a very high rate, suggesting that the two residues are not more than one water molecule apart. The correlation between these conformations and the catalytic mechanism will be discussed.

2. Materials and methods

2.1. Preparation of lac permease

The enzyme used in the present study was a generous gift of H.R. Kaback and J. Le-Coutre. The preparation was a six His-tagged enzyme, on the C terminus, Cys-less background, enzyme that was back mutated (S148C) to introduce a single cysteine at the native C148 site, reconstructing the native substrate binding site with no other maleimide binding domain on the whole enzyme. The labeling was carried out at pH 7.5 at 0°C in the dark with a final yield of 90–95% labeled protein. Before usage the protein was eluted from a P10 column by 0.018% lauryl maltoside and 100 NaCl to remove the phosphate buffer in which the enzyme was suspended.

2.2. Kinetic measurements

The kinetic measurements were carried out with solution containing pyranine (15–35 μM) and fluorescein labeled lac permease. The enzyme was suspended in 100 mM NaCl, 0.5 mM lauryl maltoside to a final concentration of 5–10 μM (with respect to the bound fluorescein) and its precise concentration was determined by its absorbance at 500 nm. The sample was placed in a four-face quartz cuvette and continuously stirred, while the pH of the solution was constantly monitored by a pH electrode. The excitation beam of the Nd:Yag laser (355 nm) and the monitoring beam of a CW Argon laser (458 nm or 496 nm) were crossing each other. The transient absorbencies were monitored at two wavelengths: at 458 nm, where the pyranine anion has an extinction coefficient of 24 000 M^{-1} cm^{-1}, and at 496 nm. During its protonation the absorbance of fluorescein at 496 nm is not totally bleached and its differential extinction coefficient (basic minus acidic) of the fluorescein is $\Delta\varepsilon\{Flu^{-}_{(basic-acidic)}\} = 50\,000$ M^{-1} cm^{-1} [23,32]. The conversion of the recorded signals to concentration accounted for the spectral contribution of each dye to the absorbance of the other at the wavelength where it was monitored. The correction values are as follows: the contribution of the fluorescein to the absorbance of the pyranine is $\Delta\varepsilon\{Flu^{-}_{(basic-acidic)}\}_{458nm} = 5000$ M^{-1} cm^{-1}, while the pyranine's absorbance at the wavelength where fluorescein was monitored was $\Delta\varepsilon\{\phi O^{-}_{(basic-acidic)}\}_{496nm} =$ 1440 M^{-1} cm^{-1}.

A train of excitation pulses irradiated the sample and care was taken to maintain the pH, during the observation period, within $\pm$0.05 unit from the initial value. After each measurement, the pH was varied by increments of 0.1–0.3 pH unit through the addition of small aliquots of NaOH or HCl (10 mM) and the measurements at the two wavelengths were repeated. The pH range used in the present study was limited between 6.0 and 8.05. At the lower end of this range, the enzyme became unstable and tended to precipitate. Measurements at the higher end of the range were limited by the ground state dissociation of the pyranine (pK = 7.7; I = 0.1 M), which depleted the ground state population of ϕOH to a level too low to perturb the system. Altogether, 56 pairs of signals (pyranine and fluorescein) were measured under varying initial conditions (pH, ratio of pyranine/enzyme, and total concentrations of reactants). All of them were subjected to

analysis and their measured signals were reconstructed in silico.

Each sample was subjected to 1000 laser pulses (1.6 mJ/pulse at a repetition rate of 10 Hz) and the transient absorbencies were measured using a Tektronix TDS 540 digital oscilloscope. The signals were stored as a vector of 15 000 data points with a temporal resolution of 2–20 ns/data point. The signals were averaged and subjected to kinetic analysis as described in the text. For a more detailed description see [24,26–28,33].

2.3. Kinetic analysis

The response of the reaction system to the pH perturbation is the summation of many parallel, tightly coupled reversible reactions that fall into two categories. The first category is the diffusion controlled reaction between the proton (or free diffusing pyranine anion) and the protein bound proton binding sites. The second mechanism is a proton exchange between the fixed proton binding sites of the protein, which proceed in a local environment where the density of the reactants, separated from each other by 3–10 Å units, is comparable to that of a homogeneous solution having a concentration of 1–4 M.

For the purpose of analysis all proton transfer reactions taking place within the perturbed space were defined and linked by equilibrium and rate equation. In principle, each of the protein proton binding site should be individually expressed, but this requirement is too demanding. In the present analysis, the system was simplified by grouping the reactive residues into subpopulations, each characterized by average equilibria and rate constants. The equilibria were converted into a set of coupled, first order, nonlinear differential rate equations that complied with the detailed balance principle and the conservation of mass [27,30,31]. The integration of these equations over time is an in silico reconstruction of the chemical reactions. With the right selection of rate constants, the integration is a reconstruction of the observed dynamics. This mode of analysis has the same rationale as the deduction of the structural model from the X-ray diffraction pattern, where a number of independent observations are reconstructed by a single set of diffracting elements placed at defined coordinates. In the same way, all the independently measured kinetic tracings that had been recorded were simulated by a single set of rate constants. To increase the accuracy of the reconstruction, the signals were analyzed in pairs, each pair consisting of the pyranine and fluorescein signals that were measured at the same pH value [26,27]. The reconstruction of the two signals, as in Fig. 3, is a summation of all parallel reactions that link the transient protonation of the moieties in the bulk, on the protein's surface, the two dye molecules and the protonable residues located inside the cavity. The mode of analysis and its results will be described in the text while the rate constants are summarized in Tables 1 and 2.

Table 1 lists the reactions of free protons with the various proton binding sites. These parameters are the minimal number of reactants needed to reconstruct the whole set of observations. In accordance with the structure proposed by Kaback and coworkers [4–7] and Brooker and coworkers [8–10], the number of exposed residues was estimated and set as the maximal number of residues that react with free protons in a diffusion controlled reaction. The cytoplasmic surface of the enzyme was efficiently represented by two populations of proton binding sites: one consisted of six carboxylates and the other of three histidine residues (it is of interest to point out that, though the enzyme was expressed with a His tag of six residues, its contribution to the proton binding dynamics of the protein was rather small). Each subpopulation was assigned an average pK value and rate constants of proton exchange with other types of proton binding sites. The periplasmic surface was also satisfactorily represented by only two subpopulations, one consisting of five carboxylates, the other of two histidine residues. Within the substrate transporting cavity, the analysis was consistent with one carboxylate (E126) and one histidine residue (H322) that were each characterized by specific rate constants, and three more carboxylates that were characterized by average values.

3. Results

3.1. Physical properties of the covalently bound fluorescein

The binding of fluorescein maleimide to C148 of lac permease shifts the absorption maximum of the anionic state of the dye from 490 ± 1 to 500 ± 2 nm, indicating that the local environment modulates the molecular orbitals of the dye (Fig. 1A). In the first singlet state, the electronic orbitals are more prone to delocalization by the intra-protein electrostatic field than in the ground state. Thus, the red shift of the absorption band of the bound fluorescein implies that the cavity provides a polarizing force that narrows the energy gap between the ground state and the excited one. Considering the proposed structure of the substrate binding site [6,12,13], it is plausible that the polarization is caused by the positive charge of R144 and the negative charge of E126 that flank the substrate from both its sides.

The pK of the bound dye was measured by monitoring the excitation spectrum of the bound dye while the pH of the solution varied gradually from 5.5 to 9.5. The results, presented in Fig. 1B, follow a smooth titration curve with an apparent pK value of $pK_{app} = 7.0 \pm 0.08$. This value is significantly higher than that of the free dye ($pK = 6.3 \pm 0.05$ at $I = 50$ mM). The slope of the titration curve is larger than 1 ($\alpha = 1.35$; $R = 0.98$), indicating that, during the titration, the protein as a polyelectrolyte responded to the pH variation by changing its surface charge during the titration. As the pH was raised, the surface became more negative with an appropriate downshift of the apparent pK. The pK shift of the bound dye is attributed to an extra stabilization of the protonated state of the dye by two forces. One is the hydrophobicity and low dielectric constant of the binding cavity, which favors the uncharged state of the dye. The second force comes from the nearby negative charges that enhance the proton attraction of the domain. Measurement of the pK of the fluorescein bound to the glutamate 126-less mutant (E126A) supports this assumption. As seen in Fig. 1B, the elimination of the charge caused a small but systematic shift of the titration curve to slightly lower values, indicating that the immediate vicinity of the dye is less negatively charged.

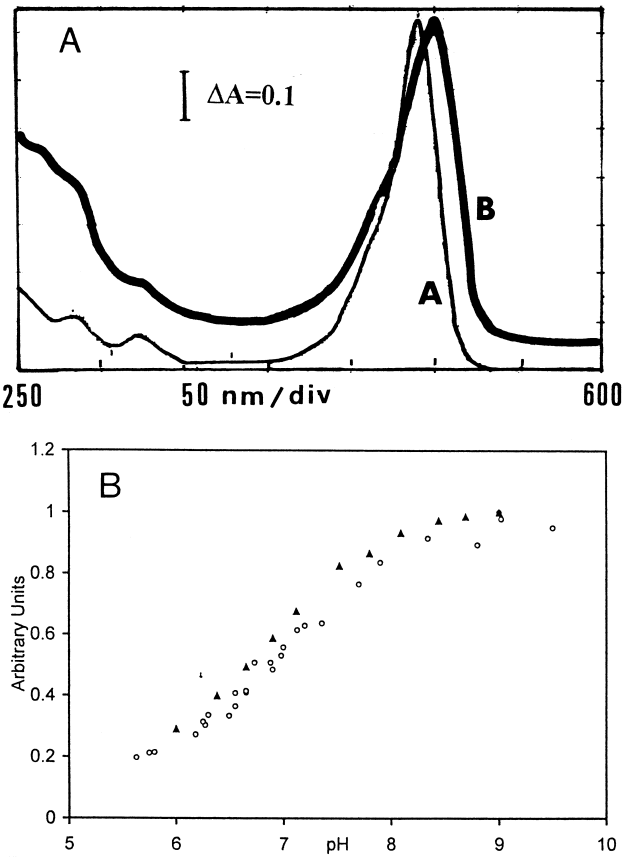

Fig. 1. Absorption spectra of the C148–fluorescein maleimide adduct of lac permease and its pH titration curve. Panel A depicts the absorption spectra of the alkaline state of free fluorescein (4.7 μM, pH 8.0) (line A), and of the fluorescein–lac permease adduct (line B). For the sake of clarity, line B was shifted upwards with respect to line A. The maxima of the two spectra are at 493 and 500 nm respectively. Panel B depicts the pH titration curves while monitoring the fluorescence (excitation at 500 nm, emission at 515 nm) of the fluorescein C148–lac permease adduct (○) and of the adduct with a protein where E126 was mutated to alanine (E126A; ▲). Please note that the systematic shift of these data points to lower pH values. The titrations were carried out in 0.5 μM lac permease in 100 mM KCl, 5 mM Tris–MES buffer.

3.2. Protonation kinetics of free and bound fluorescein

The dynamics of the acid–base perturbation, imposed during a proton pulse experiment, are demonstrated in Fig. 2. The protons, discharged from the excited pyranine molecule, are released within the response time of the measuring system, and an equal quantity of free protons and pyranine anion is formed. The protons react with the pyranine anion

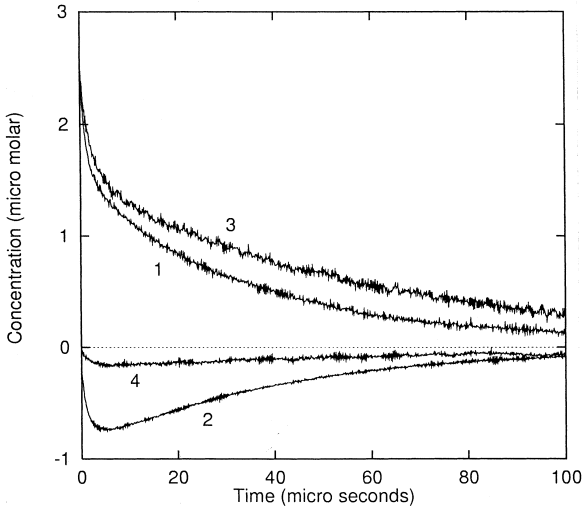

Fig. 2. Transient absorbencies associated with acid–base perturbation of pyranine and fluorescein in solution. The experiments were carried out with pyranine (29 μM) and either free fluorescein (9 μM) (curves 1 and 2) or fluorescein labeled lac permease (9 μM with respect to the bound fluorescein, curves 3 and 4). The measurements were carried out in 100 mM KCl at pH 7.70. The upper two curves were measured at 458 nm and record the re-protonation of the pyranine anion. The bottom curves were measured at 496 nm and monitor the reversible bleaching of the fluorescein chromophore due to its protonation.

(curve 1) and with the fluorescein (curve 2) in a diffusion-controlled reaction. During the first phase of the reaction, lasting approx. 5 μs, both dyes react with the free protons and reduce their concentration to an almost pre-pulse level [27,28]. At a later phase ($t > 5$ μs), the relaxation proceeds by a collisional proton transfer, where the rate limiting step is the encounter between a protonated fluorescein molecule and a pyranine anion. This mechanism is evident from the mirror symmetry of the relaxing curves; all protons not present on the pyranine (curve 1) reside on the protonated fluorescein molecules (curve 2).

Repeating the same measurements with a protein bound fluorescein generates a different kind of relaxation curve (Fig. 2, curves 3 and 4). The protein, with its many proton binding sites, competes with the pyranine for the free protons and the rapid phase of pyranine re-protonation is missing. What is more, as the protons are bound to the protein, the main mechanism of relaxation is a collisional proton transfer from the protonated site on the protein with a free diffusing pyranine anion. This modulation of the pyranine transient is the kinetic signature of the protein buffers' capacity [26,27,30]. The pyranine signals measured with the native lac permease or with the fluorescein adduct were identical within the limit set by the electronic noise, indicating that the fluorescein residue makes a minor contribution to the total buffer capacity of the protein and that its binding does not modulate the structure of the protein in a way that affects its proton binding capacity.

The dynamics of fluorescein, bound to lac permease, are characterized by fast rise and slow relaxation times. The fast protonation indicates that the protein facilitates the access of proton to the dye, while the slow relaxation suggests that the presence of a local proton reservoir replenishes the dye with protons. Accordingly, the reconstruction of the dye's dynamics should account for these processes.

3.3. Effect of pH on the protonation dynamics

The velocity of a chemical reaction is a function of the reactants' initial concentrations. Accordingly, variation of the pre-pulse [ionized]/[protonated] ratio of the reactants through modulation of the pH should affect the velocity of the proton transfer reactions that follow the pH jump. For this reason, the kinetic measurements were repeated at varying initial pH values and the dependence of the reaction on the pH was investigated. However, the procedure is limited to a certain pH range. At $pH > pK_0^{\phi OH}$ the concentration of the ϕOH species decreases and a smaller perturbation is expected. Similarly, at $pH < pK_{(flu)}$ the dye will mostly be in its protonated state and the incremental protonation, in response to the proton pulse, will diminish.

Fig. 3 depicts a set of kinetic measurements carried out at varying initial pH values. Fig. 3A depicts the pyranine relaxation signals as they vary with the initial pH. As the pH increased from 6.0 to 8.03, the initial ϕOH population decreased, reducing the amount of protons released by the laser pulse (Fig. 3A). The pH also affected the shape of the curve, and at high pH values a slower phase appears, representing an increment in the protein's buffer capacity.

The fluorescein signals retain their general shape over the whole pH range, even when below 7.2 its relaxation is faster than at the higher pH range (com-

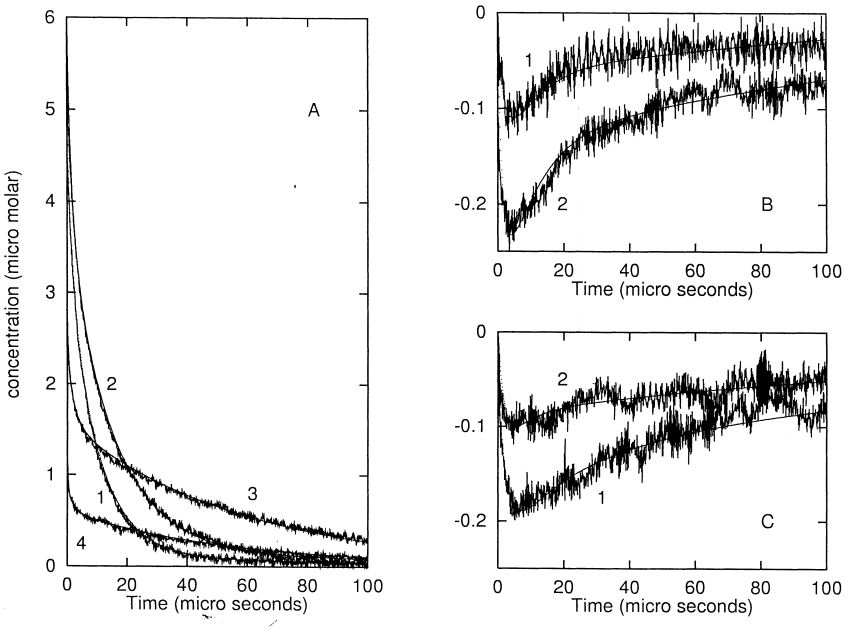

Fig. 3. The effect of the pre-pulse pH on the protonation dynamics of labeled lac permease. The experiments were carried out in 100 mM KCl, 29 μM pyranine and 9 μM of fluorescein–lac permease. The transients shown in panel A were recorded at 458 nm and the pre-pulse pH of the solution, where curves 1, 2, 3 and 4 were measured, was 6.0, 6.6, 7.45 and 8.03 respectively. Panels B and C depict the transient protonation of the bound fluorescein measured at pH 6.0 and 6.3 (curves 1 and 2 in panel B). Panel C depicts the fluorescein protonation curves as measured at pH 7.45 and 8.03 (curves 1 and 2, respectively). Each pair of curves is presented with its simulated dynamics, which is the continuous line superpositioned over the experimental one. The set of rate constants that reconstructs the observed dynamics is given in Tables 1 and 2. Please note the different scale of the ordinate corresponding to the fluorescein signal.

pare Fig. 3B and C). The initial pH also affected the amount of fluorescein protonated during the perturbation. As the pH increased, the maximal yield of protonated fluorescein, normalized with respect to the increment of ϕO^-, increased from 3.2% at pH 6.0 to 9% at pH 8.03. This enhancement is surprising considering the enhanced proton binding capacity of the protein and an approx. 40-fold increment in the ground state ϕO^- population. To account for the enhanced reactivity of the fluorescein at higher pH values, it was suspected that the mechanism of the bound fluorescein protonation varies with the pH, thus necessitating a precise kinetic analysis of the signals.

3.4. Numeric reconstruction of the measured transients

The manifold shapes of the relaxation dynamics, as shown in Fig. 3, can be reconstructed by a set of coupled non-linear, first order, differential rate equations that comply with the detailed balance principle [19,22,34,35]. The equations account for all proton transfer reactions between each component $\{R_i\}$ and each of the other proton binding sites $\{R_j\}$ present in the system as given by Eq. 1.

$$dR_i/dt = k_{diss}\{RH_i\} - k_{as}\{R_i\}\{H^+\} + \Sigma k_{ji}\{RH_i\}\{R_j\} - \Sigma k_{ji}\{R_i\}\{RH_j\} \quad (1)$$

The term k_{diss} corresponds with the rate constant of the acid dissociation of RH_i; k_{as} is the re-protonation of R_i; $\Sigma k_{ji}\{RH_i\}\{R_j\}$ is the sum of all reactions where $\{RH_i\}$ functions as a proton donor to other proton binding sites, and $\Sigma k_{ji}\{R_i\}\{RH_j\}$ is the sum of the back-reaction where $\{R_i\}$ is the acceptor with respect to all other proton binding sites. The same equations, with the appropriate rate constants, are given for each reactant in the system and are linked in a model that ensured the mass conservation law. Numeric integration of the whole set of the equations is the mathematical equivalent of the

chemical reaction. When the equations are supplied with the correct values of the rate constants, the computer generated dynamics will reconstruct the measured reactions. The reconstruction of a single pair of measured dynamics has a large leeway in the selection of rate constants. Yet, as the number of independent, non-identical signals increases, the solutions converge to a single set of rate constants that solves all experimental results. Recent application of a genetic algorithm procedure for proton pulse measurements, with 12 independent adjustable parameters, indicated that the system converges to a single global minimum (Fibich and Nachliel, unpublished results).

The implementation of the differential rate equations for the lac permease–fluorescein adduct necessitates definition of the various proton binding sites involved in the reaction. Naturally, accounting for each of the proton binding residues is a precise presentation of the system, but the penalty would be an overwhelming increment in the complexity of the system. For this reason, the number of independent proton binding sites that were included in the numeric reconstruction was reduced as described below.

1. The two dyes, pyranine (ϕOH) and fluorescein (Flu), were explicitly presented by their formal concentrations.
2. The proton binding sites on the periplasmic side of the protein were grouped into two subpopulations: the carboxylates $(COO^-_{av})_{pri}$ and the histidines $(His_{av})_{pri}$. The number of elements (n_i) in each subpopulation was an adjustable parameter with the limitation $n_i \leq n_{max,}$ where n_{max} is the number of residues on the surface as estimated by Kaback's structural model [5].
3. The proton binding sites on the cytoplasmic side of the protein were grouped into two subpopulations; the carboxylates $(COO^-_{av})_{cyt}$ and the histidines $(His_{av})_{cyt}$. The number of elements in each subpopulation was an adjustable parameter as described above.
4. The intra-protein proton binding sites were equated with the reactive residues identified by Kaback and coworkers [5] as essential for the enzymic activity; histidine (H322) was treated explicitly while the four carboxylates were split into two subpopulations. The effects of the E126A mutation on the apparent pK of the bound fluorescein suggested some coupling between the two proton binding sites. Accordingly, one of the intra-protein carboxylates was treated as an explicit group (COO^-_{E126}), while the other carboxylates were grouped in one subpopulation (COO^-_{in}) that was assigned by average parameters. Because of their high pK, the lysine and arginine moieties were assumed to be constantly protonated and made

Table 1
The kinetic and thermodynamic parameters of the reactions of free diffusing protons with proton binding sites on lac permease

	Reaction	n	pH <7.1		pH >7.4	
			Rate constant	pK	Rate constant	pK
Cytoplasmic surface						
1	**$H^+ + COO^-_{av}$**	6	**3×10^9**	**4.0**	**7×10^9**	**4.2**
2	$H^+ + His_{av}$	3	1×10^9	6.3	1×10^9	6.3
3	$His_{av} + \phi O^-$	3	1.5×10^8		1.5×10^8	
Periplasmic surface						
4	$H^+ + COO^-_{av}$	5	1×10^9	4.8	1×10^9	4.8
5	**$H^+ + His_{av}$**	2	1×10^9	**7.5**	1×10^9	**7.1**
6	$His_{av}H^+\phi O^-$	2	1.5×10^8		1.5×10^8	
Protonation of intra-cavity residues						
7	**$H^+ +$ Fluorescein**	1	**10×10^9**	7.0	**2.5×10^9**	7.0
8	**$H^+ + COO^-_{E126}$**	1	**1×10^9**	5.7	**2.5×10^9**	5.75
9	$H^+ + His_{H322}$	1	1×10^9	7.3	1×10^9	7.3
10	$H^+ + COO^-_{av}$	3	1×10^9	5.0	1×10^9	5.0

All rate constants are given in M^{-1} s^{-1} units. Bold face reactions vary in their parameters when the pre-pulse pH shifts between the high and low pH regimes. The value n represents the number of residues per protein.

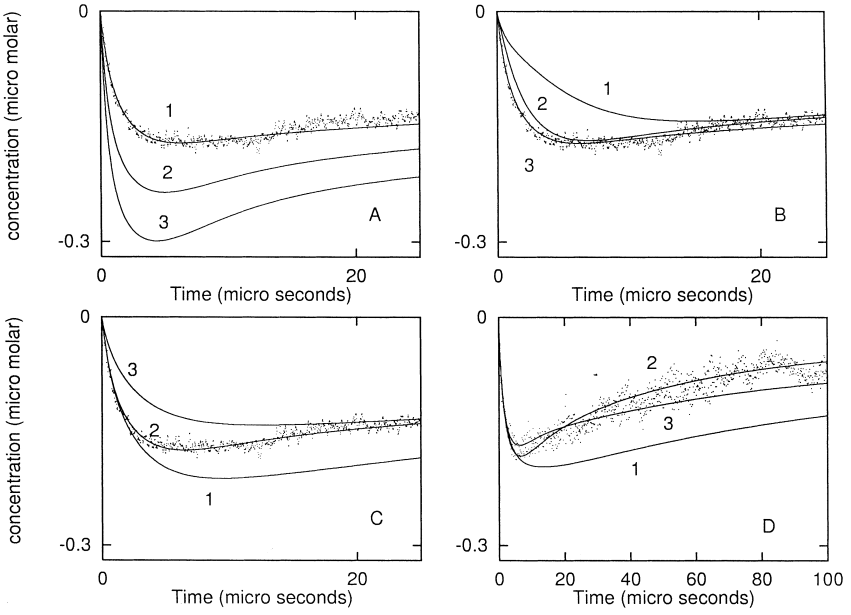

Fig. 4. The effects of the rate constants on the observed dynamics. The curves in each panel were generated by the parameters given in Tables 1 and 2 except for one parameter which was varied within the indicated range, as given below. For comparative purposes a fluorescein signal (measured at pH = 7.45, 100 mM KCl, 19 μM pyranine, 9 μM covalently bound fluorescein) is presented by the experimental points. Panel A depicts the effect of the rate of reaction between the dye and free diffusing protons (Line 1. $k = 2.10^{9-1}s^{-1}$; line 2. $k = 6.10^{9}M^{-1}s^{-1}$; line 3. $k = 1.10^{10}$ $M^{-1}s^{-1}$). Panel B demonstrates the effect of the 'virtual second order' rate constant of proton transfer between the E126 carboxylate and the bound fluorescein (line 1, 1.10^{10}; line 2, 1.10^{11}; line 3, 2.10^{12}). Panel C depicts reconstructed dynamics where the proton exchange rate between histidine 322 and the fluorescein was modulated (line 1, 2.10^{9}; line 2, 6. 10^{9}; line 3, 1.10^{10}). Panel D corresponds with the dynamics calculated for three pK values of histidine 322 (line 1, pK = 7; line 2, pK = 7.3; line 3, pK = 7.6).

no contribution to the buffer capacity of the protein.

All proton binding sites were assigned rate constants for their reactions with free protons, freely diffusing pyranine anion and proton exchange reactions with all other proton binding sites. The distinction between the sites located on the periplasmic vs. the cytoplasmic side was attained by setting ($k_{j/i} = 0$) for all proton exchange between groups located on opposite faces of the enzyme.

The set of parameters that reconstructs the experimental system made of pyranine and the fluorescein–lac permease adduct, over the whole pH range, is given in Tables 1, 2 and 3. The quality of the reconstructed dynamics is demonstrated by the deviation plots (insets to Fig. 6 below). Along the full length of the observation time, neither the pyranine nor the fluorescein reconstruction exhibits a systematic deviation from the experimental data.

3.5. Reconstruction of the pyranine signals

The relaxation of the pyranine anion is regulated by the total buffer capacity of the protein, to which the fluorescein makes a negligible contribution. As a result, the relaxation of the pyranine signal is affected by the concentration of the protein's proton binding sites and their pK values. An attempt to simulate the pyranine signals, assuming that all histidine residues of the His tag reacted with free proton in a diffusion controlled reaction, failed to fit the observations. The number of histidine residues on the cytoplasmic surface that participate in the microsecond proton uptake reactions had to be adjusted to three. By the same reasoning, the number of histidine residues on the periplasmic face was set to be two. It seems that a combination of steric hindrance and interaction between the surface groups reduces the number of residues on the enzyme's surface which are capable of reacting with

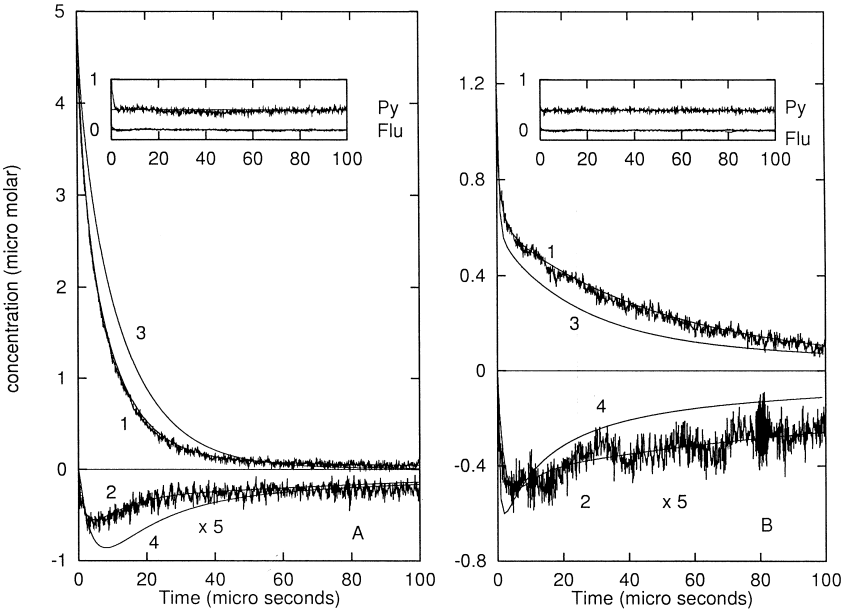

Fig. 5. Reconstruction of the measured dynamics by the rate constants of the high and low pH regimes. Panel A depicts the dynamics measured at pH 6.0 with its reconstructed dynamics. Lines 3 and 4 were calculated with the parameters adequate for the high pH regime. Lines 1 and 2 were reconstructed by parameters that were fitted for the low pH regime. The quality of the fitting is recorded in the inset. Panel B depicts the kinetics measured at pH 8.03. Lines 3 and 4 were calculated with the parameters suitable for the low pH regime. Lines 1 and 2 were calculated with the parameters of the high pH regime and the quality of the fit is recorded in the inset. In the two insets, for sake of clarity, the plots for the fluorescein and pyranine were shifted along the *Y* axis. Please note the different ordinate scale used for the fluorescein signals.

the free proton within the 2 μs time frame, where the free proton concentration exceeds the pre-pulse level [23,24,26,27].

The reconstruction of the experimental pyranine signal, over the pH range, was essentially attained by the same parameters (see Table 1) except for two: the rate of protonation of the average carboxylate population of the cytoplasmic face of the enzyme, and the p*K* of the average histidine residues on the periplasmic side. Both parameters were found to

Table 2
The virtual second order reaction of proton exchange between the proton binding sites of lac permease

		pH <7.1	pH >7.4
Reaction on the cytoplasmic surface			
1	$COOH_{av} \rightarrow His_{av}$	1×10^9	2×10^9
Reaction on the periplasmic surface			
2	$COOH_{av} \rightarrow His_{av}$	10×10^9	10×10^9
Cytoplasmic → cavity			
3	$COOH \rightarrow COO^-_{E126}$	10×10^9	8×10^9
4	$His_{av}H^+ \rightarrow His_{H322}$	***10×10⁹***	***Negligible***
Periplasmic → cavity			
5	**$COOH_{av} \rightarrow$ fluorescein**	***7.5×10⁹***	***Negligible***
6	**$COOH_{av} \rightarrow His_{H322}$**	***1×10⁹***	***10×10⁹***
7	**$His_{av}H^+ \rightarrow His_{H322}$**	***0.1×10⁹***	***1×10⁹***
Intra-cavity proton transfer			
8	**$COOH_{E126} \rightarrow$ fluorescein**	***$k<10^7$***	***2.5×10¹²***
9	**Fluorescein H $\rightarrow His_{H322}$**	***5×10⁹***	***2.5×10⁹***

Bold face reactions vary in their parameters when the pre-pulse pH shifts between the high and low pH regimes.

vary between the two pH regimes in a range beyond the limit of confidence in the analysis.

3.6. Reconstruction of the fluorescein signals

The reconstruction of a single pair of tracings can be obtained by more than one combination of the rate constants. Yet, as the number of independent observations increases, the range of variance of the rate constants converges. The limits of variance of each parameter are given in Tables 1–3. In a case where one parameter exceeds its boundary, the whole set of measured signals cannot be reconstructed even if all the other parameters are allowed to vary.

The protonation of the fluorescein is a summation of two processes: reactions of the dye with free diffusing species (protons and pyranine anion) and proton exchange between protonable residues located within approx. 20 Å from the dye [19,27,28]. The shape and amplitude of the fluorescein signal are mostly controlled by the parameters presented in Fig. 4. Each frame in the figure depicts the reconstructed dynamics (measured at pH 7.45), where one parameter varies within the indicated range. The rate constant that mostly affects the amplitude and initial velocity of the reaction is the protonation of the fluorescein by free diffusing protons. In Fig. 4A, the well-fitted curve was calculated with $k = 2 \times 10^9$ M^{-1} s^{-1}. This value is significantly smaller than a rate constant of a diffusion controlled reaction. Attempts to reconstruct the signal with larger rate constants caused gross deviation from the experimental curve. The slow protonation of the bound dye indicates limited accessibility of protons to the substrate binding cleft of the enzyme.

Fig. 4B demonstrates how the intra-protein proton exchange with E126 affects the fluorescein signal. The variation of the rate constant from 2×10^{12} (characteristic to proton exchange between sites that are less than 10 Å apart) to 1×10^{10} affects both the amplitude and its evolution with time. The quality of the measured signal is good enough to establish that the rate constant of the reaction is $k \approx 10^{12}$. The rapid accumulation of the protonated dye is a consequence of a rapid shuttle mechanism, where the carboxylate of residue E126 delivers proton to the dye.

The effect of proton exchange between the fluorescein and the intra-cavity histidine (H322) is shown in Fig. 4C. In contrast to the proton exchange between the carboxylate and the fluorescein, the proton transfer reaction between the dye and the nearby histidine is much slower, and the best fit was calculated with $k = 2 \times 10^9$. Thus, at pH ≥ 7.4, the mechanism of proton exchange with the histidine is less efficient than with E126. The shape of the fluorescein relaxation curve is very sensitive to the pK value assigned to histidine residue H322 (Fig. 4D). The best estimation, based on analysis of 27 independent measurements, is p$K = 7.3 \pm 0.08$.

3.7. Effect of pH on the lac permease conformation

To obtain a large number of experimental tracings, with varying protein/pyranine ratios, the experiments were carried out within the pH range $6.0 \leq$ pH ≤ 8.0, where good quality data could be obtained. Altogether 56 pairs of signals were recorded. The analysis of the signals was carried out, starting with those gathered at the high pH range, and proceeding systematically to the lower pH values. In the pH range of 8.1–7.4, we analyzed 27 pairs of signals that were all solved by one set of parameters. When the same solution was tested on signals measured at pH ≤ 7.1 (see Fig. 5A, curves 1 and 2), they totally failed to resemble the shape of the curve. Fig. 5A presents the experimental signal measured at pH 6.0 together with two reconstructed dynamics. The reconstructed curves (lines 3 and 4, for pyranine and fluorescein respectively) were generated by parameters suitable for the results gathered above pH 7.4, and grossly deviate from the experimental data. It is obvious that these parameters are inadequate to reconstruct the transients in the low pH regime. A new set of parameters should therefore be searched for. The results of 29 kinetic measurements, obtained below pH 7.1, were subjected to kinetic analysis and a new set of rate constants was obtained. These parameters were appropriate to reproduce the results of the low pH regime (see Fig. 5A, lines 1 and 2 and the deviation plot in the inset). The new set of parameters was found to be inadequate for the reconstruction of the signals gathered at high pH range (see Fig. 5B, lines 1 and 2). Thus we conclude that the proton

pulse measurements revealed two states of the enzyme, each having its own kinetic parameters for reaction with free protons.

The transition between the two conformations was very sharp. Up to pH 7.1, all measurements could be fitted by the parameters of the low pH regime, while above 7.4 all observations were simulated by the other set of parameters. In the intermediate range, the two conformations coexisted and the signals could not be fitted by either set. The two sets of solutions are given in Tables 1 and 2 and the difference between them is sufficiently large to associate each solution with a different conformation of the enzyme.

3.8. Quantitative evaluation of the rate constants

3.8.1. Interaction of free protons with the protein's surface

The following tables summarize the pK values and rate constants associated with the reversible protonation of the fluorescein maleimide attached to C148 of the lac permease, and reflect the combined features of the covalently bound dye and residues of the substrate binding site. Table 1 lists the rate constants of the diffusion-controlled reactions between the various residues with free diffusing species (H^+ and ϕO^-). The reactive groups are defined in the first column. The two chromophores and the intra-protein residues E126 and H322 are marked as such, while the others are labeled with generic names (like His_{ave} etc.) The properties of the imidazole residue of H322 were assigned to the high pK intracavity residue that regulated the decay dynamics of the fluorescein (see Fig. 4C,D). The kinetic features of the E126 carboxylate were corroborated upon analysis of the cysteine-less/C148/E126A double mutant (see Fig. 5). The number of residues in each subpopulation is given in the second column. It should be pointed out that the number of residues was equal, or smaller, than the estimation based on the structure proposed by Kaback [5]. Taking the full content of histidine residues, including the His tag groups, yielded a proton binding capacity too high to fit the measured signals. The reconstruction of the signals was attained with only three, fast reacting histidine and six carboxylate residues.

The other four columns in Table 1 refer to the rate constants of protonation and the pK of each subpopulation when the protein is either above pH 7.4 or below 7.1 (the high and low pH regimes, respectively).

Of all reactions with the free proton, only that of the fluorescein, in the low pH regime, is fast enough to comply with the diffusion controlled reaction. All other reactions are smaller than 1×10^{10} M^{-1} s^{-1}, a value measured for exposed residues on other proteins [23,24,26–28,30] or for phosphatidylserine in a lipid membrane [31]. Apparently, the surface carboxylates of lac permease are well shielded from reaction with bulk protons either by adjacent positive residues or partial insertion in a non-polar environment. The slow reaction of the surface groups with free protons cannot be attributed to the presence of the supporting lauryl maltoside micelles as the same phenomenon has been found with lac permease in lipid vesicles (Nachliel, unpublished results). Furthermore, the surface groups of cytochrome oxidase [26,27], stabilized by the same concentrations of lauryl maltoside, reacted with free protons at rate constants compatible with the Debye–Smoluchowski equation ($k > 10^{10}$ M^{-1} s^{-1}).

The rate constant values listed in bold letters in Table 1 merit special attention, as they differ markedly in the high and the low pH regimes. The most prominent value is the protonation of the bound fluorescein. In the low pH range, this rate constant is compatible with that of the diffusion controlled reaction, indicating that the cleft where the dye is bound is fully exposed to the bulk. (Kinetic analysis cannot determine whether the opening is towards the extracellular space or on the periplasmic side of the protein.) In the high pH range, the reaction is 4 times slower, suggesting that the cavity closed over the bound dye thus barring the free entry of protons into the cleft. In contrast to the fluorescein, the protonation of E126 and the cytoplasmic surface carboxylates is faster in the high pH regime. Thus, the effect of the pH on the accessibility of the proton binding sites exhibits site selectivity and is not a general property of the protein.

On the periplasmic side of the protein, the rate constants are pH-insensitive but the pK of the histidine residues varies between the two conformations of lac permease. As evident from these data, the transition of the protein from one conformation to

the other appears to be selective, and the various proton binding sites respond independently to the transition.

Finally, we wish to emphasize that, although the p*K* values of the carboxylates as listed in Table 1 are lower than the pH range where the measurements were carried out, their value was determined with high accuracy. This confidence is gained from the mode by which the p*K* is derived. Unlike equilibrium titration, where the p*K* is measured by counting the fraction of the population that is protonated at a given pH, in the kinetic analysis the p*K* is determined by the ratio of the rate constants for the reversible protonation of the residue. As both rate constants are independent, adjustable parameters, the p*K* can be derived even when the system is far from its state of equilibrium.

3.8.2. Proton transfer between fixed sites

The carboxylate and histidine residues of lac permease are rigidly fixed on the scaffolding of the protein and cannot diffuse one from the other. Still, these residues can rapidly exchange protons amongst them at a very fast rate. The probability and the rate of proton exchange between surface sites are a function of the nearest approach between them and the frequency at which they reach that transient configuration. The reactions under these conditions are reminiscent of proton dissociation in water, except that the acceptor is not the water molecules but the local proton acceptor that acts as the solvent. When the local transient conditions are favorable, the proton transfer reaction to the acceptor can be faster than the dissociation reaction, especially in a micro-cavity where the activity of the water can be small [36]. Studies with model systems established that the rate constant of proton exchange between sites anchored on a rigid body could be expressed by a 'virtual second order rate constant' [27] and their values can be as high as 10^{12}. These rate constants appeared to be proportional to the distance between the donor and acceptor sites, as well as their state of solvation and the electrostatic potential in the most immediate vicinity [27]. On the other hand, due to the virtuality of the concentration term used in the calculation, the M^{-1} s^{-1} unit cannot be assigned to these rate constants. In the present text, all virtual second order rate constants are printed in italics. As a rule, when two residues exchange protons at a rate of 10^{12}, the two sites are separated by either one or two water molecules, which facilitate rapid proton exchange between them. When the virtual rate constant is approx. 10^{9}, the two sites are 10–15 Å apart, or a positive charge is inserted into the proton transfer trajectory. A slower virtual rate constant implies that the mechanism of the reaction is dissociation, followed by random diffusion until the proton encounter with the acceptor site.

The virtual rate constants measured for the proton transfer reactions in the fluorescein labeled lac permease are listed in Table 2 and those values that exhibit a major variation to the pH regime are printed in bold. The most dramatic diminution of a virtual rate constant was noted for the proton transfer from the intra-cavity carboxylate, identified as E126, and the bound fluorescein (reaction 8, Table 2). As demonstrated by the reconstruction (Fig. 4B), the rate of this reaction controls the velocity of the protonation of the bound fluorescein. The mechanism supporting this fast reaction is proton transfer from the nearby carboxylate (E126) that shuttles the protons from the bulk to the dye. The reconstructions presented in Fig. 4B indicate that the rate constant of the reaction, in the high pH regime, is 10^{12}. In the low pH range, the same rate constant of proton is slowed by a factor of 100 000, indicating that the connectivity between the two sites is lost.

The other intra-protein proton transfer reaction is the proton exchange between the fluorescein and the high p*K* residue located in the cleft (reaction 9). The virtual rate constant of the reaction is approx. 1000-fold slower than the one with the E126 and less sensitive to the conformation change. Thus, the transition between the two conformations does not affect all intra-cavity proton transfer to the same extent.

The other virtual rate constant of proton transfer, in which H322 is involved, also varies between the two pH regimes, indicating that the conformation change is not just limited to helix IV, that carries E126, but is widespread over various domains of the protein.

3.9. Positive identification of E126 by its kinetic features

The kinetic analysis indicated that a single carbox-

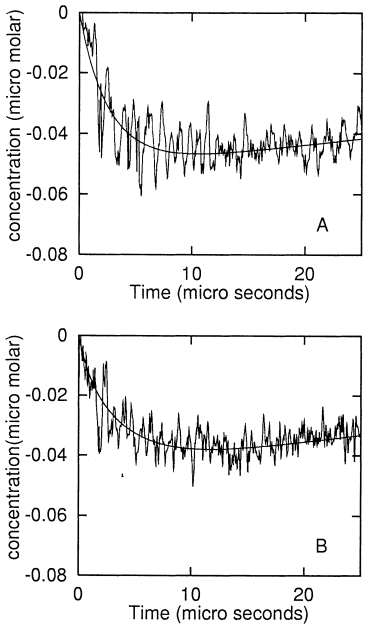

Fig. 6. Experimental results and their reconstructed curves measured for the fluorescein adduct with the Cys-less background E126A/S148C double mutant. The measurements were carried out in 100 mM KCl, 30 μM pyranine and 0.9 μM of the bound fluorescein. Panels A and B correspond with the dynamics measured at pH 6.85 and 7.65, respectively. The reconstructions of both curves are based on the rate constants of the low pH regime with the modifications given in Table 3.

ylate residue is located at very close proximity to the bound indicator and facilitates its protonation. Of the four carboxylates located in the transmembrane section of the protein, E126 has been implicated as the residue which mostly interacts with the transported galactosides [37,38]. For this reason, the kinetic properties of the cysteine-less/C148/E126A mutant were investigated.

The reprotonation of the pyranine, measured with the E126A mutant, was indistinguishable from that measured above, in accordance with the minor contribution of E126 to the total proton binding capacity. On the other hand, the kinetic analysis of the protonation dynamics of the fluorescein (Fig. 6) failed to reveal the transition between the two pH regimes. The analysis of the signals measured at pH 6.85 was based on the parameters of the low pH regime, while setting the rate constants of all proton transfer reactions in which E126 is a reactant to zero ($k_{i/j} = 0$). The parameters that reconstruct the signals measured with the E126 mutant are given in Table 3.

At the high pH range, the amplitude of the fluorescein signal measured with the E126A mutant was found to be smaller than at pH 6.85, in contrast to those measured with the E126 enzyme (see Fig. 3), where the amplitude increased in the high pH regime. The reduced, protonation of the dye indicated that the proton shuttle pathway via E126, which sustains the high flux above pH 7.4, is indeed missing in the mutant. The reconstruction of the curve, shown in Fig. 6B, was attained by the rate constants used for the reconstruction of the low pH conformation of the enzyme, except that the accessibility of free protons to the bound fluorescein was reduced to approx. 50%, while in the parent protein the rate of the reaction was slowed, with the pH change, to 25% of the rate in the low pH regime. The rate constant of proton exchange between the bound fluorescein and H322 was found to vary with the pH, having the same values as in the E126/C128 fluorescein. Thus, the E126A mutant retains the pH dependent regime but the absence of the proton shuttle mechanism alters the protonation dynamics of the dye in the substrate binding cavity. We conclude that the carboxylate of E126 is crucial to the protein–substrate interaction but does not trigger the conformation change.

Table 3
Comparison of the proton transfer kinetic parameters that vary with the pH upon mutating E126 to E126A

Reaction	E126		E126A	
	pH <7.1	pH >7.4	pH <7.1	pH >7.4
$COO_{E126}H+Flu$	$k<10^7$	2.5×10^{12}	$k=0$	$k=0$
$Flu+H^+$	1.0×10^{10}	0.25×10^{10}	1.5×10^{10}	0.8×10^{10}
$FluH+His_{H322}$	5×10^9	2.5×10^9	5×10^9	2.5×10^9

4. Discussion

The lac permease functions as an enzyme that utilizes the electrochemical gradient of protons built across the bacterial inner membrane for the accumulation of substrate. The reaction with the two substrates (lactose and proton) is coupled and reversible; thus the enzyme can build up a proton gradient at the expense of unequal substrate concentrations. To carry out these reactions, the enzyme should exist in at least four major configurations. Two of them represent the different protonation states of the enzyme, while the other two differ in their affinity to the substrate. The catalytic cycle alternates between states where the stabilization of the substrate is attained by strong interaction with ligand groups of the protein, and those where water penetrates to the binding cavity and replaces the protein's ligands by hydrogen bonds with the water molecules. The transition between these two states is controlled by the state of protonation of the enzyme [7,8,37,38]. According to a recent study where the effect of pH on the substrate binding was measured, it seems that the affinity of the site to the substrate decreases with the pH. Upon replacement of H322 by an unprotonable residue, the binding was significantly weakened and became pH independent [39]. While Kaback and coworkers [39] quantitated the accessibility of a substrate analogue to the site by measuring its capacity to protect C148 from reacting with *N*-ethylmaleimide, in the present study the site is irreversibly labeled by fluorescein maleimide and the accessibility of proton to the site was determined by real-time kinetic measurements. Accordingly, the measured parameters are not identical but may converge to the same conclusions.

The present studies were carried out with lac permease stabilized in the micellar system: thus both sides of the enzyme were exposed to the same pH. Yet, as the enzyme maintains a leak-proof proton seal, any event that is driven by selective protonation of a site which is not accessible from both sides of the protein will affect the observations just as a membrane embedded enzyme. On the basis of kinetic analysis, we concluded that below pH 7.1 the substrate binding cleft is fully exposed to bulk protons, residue E126 is partially inaccessible to the bulk and, as evaluated by the rate constant of proton exchange between the carboxylate and the chromophore, the connectivity between the bound dye and E126 is rather weak. Based on these characteristics, the low pH state of the enzyme is compatible with a configuration where the cleft is well-solvated and the substrate about to be released to the bulk. The results of Sahin [39] suggest that, in the low pH regime, the accessibility of the substrate analogue to the site is high and 0.1 mM of TDG suffices to protect the cysteine from reacting with the maleimide.

The second state of the enzyme, favored at pH $\geq$7.4, is characterized by a closed cleft and high proximity of the E126 carboxylate (on helix IV) to the dye. In the high pH state, the two residues exchange a proton among them with a virtual rate constant of 10^{12}. This state of the enzyme corresponds with the tight complex where the intra-cavity polar groups fold on the substrate and hold it tight. In this configuration [39], the interaction between H322 and a substrate analogue is weakened, thus resembling our observation that the rate constant of proton exchange between the dye and H322 is halved. It is of interest to point out that the two pH regimes, measured in the present case by the proton accessibility to a dye molecule attached to C148, were also noted by the group of Kaback [39] (pK = 8.1). Yet, as the mode of detection varied between the two modes of observation, the pH range and transition are not identical. Thus the two modes of observation corroborate each other.

During the catalytic cycle, some of the helixes interact with the substrate in an alternating mode [40–43]. The involvement of helix IV in the process may be deduced by the alternating accessibility of E126 to the bulk. In the high pH configuration, the fluorescein is secluded from the bulk, but E126 is better exposed to reaction with bulk protons. This observation might suggest that the major proton pathway to the bound fluorescein is through the side antipodal to E126, i.e. the periplasmic one. In the low pH state, the fluorescein (bound to the substrate anchoring C148) is the better exposed moiety, while the E126 reaction with free protons is 4 times slower than in the high pH state. This inverse relationship may reflect a variation in the solvation of microdomains inside the substrate conducting pathway and corroborates the scissor mechanism of Kaback [5,6]. In a previous publication [36] we reported that an intra-

protein space of lac permease indeed exhibits a variation in solvation during conformation changes of the protein.

According to current molecular models, the galactose in its bound state appears to be sandwiched between helix V and helix IV where residues C148, M145 (both on helix V [12,13]) and E126 and R144 (on helix IV [37,40]) seal it from all sides (see Fig. 5 in [5]). In that state, the glucosyl and galactosyl residues and the oxygen atom that links them are roughly on the same plane. The fluorescein molecule with the planar xanthene chromophore has a molecular weight comparable to that of the galactose (342 vs. 427, respectively). When the fluorescein is anchored by a C–S covalent bond with the C148 sulfur atom in the substrate conducting cavity, it may assume a position similar to that of the substrate. This location is in accord with the spectral red shift of the dye (Fig. 1), as caused by the polarizing field generated by the positive (R144) and negative (E126) residues in the cavity. Naturally, due to the rigidity and planarity of the xanthene structure, plus the bulkiness of the benzoic acid-maleimide residue of the fluorescein maleimide, the fitting of the dye inside the cavity is not identical to that of the substrate and some distortion of the protein's structure is expected. However, kinetic evidence for the involvement of E126 in the protonation of the fluorescein supports the proposed location of the dye.

The experiments we carried out indicate that the fluorescein–lac permease complex retains the structural flexibility of the native enzyme. The protein can alternate reversibly between two conformations. One conformation, dominating in the low pH regime, has an open cleft structure and protons react with the chromophore in a diffusion controlled reaction. As the pH is raised, the other conformation appears. The transition between the two states is within 0.5 pH unit. Such a steep shift between the conformers suggests a cooperative interaction, similar to that proposed by Kaback [38] and Brooker and coworkers [41] between residues that trigger the transition.

According to the current models of the catalytic cycle [39], the transition between the two states is tightly associated with the substrate pumping mechanism. The active transport by lac permease, as shown by Kaback and coworkers [42,43], has a sharp maximum at pH 7.0–7.5. This pH range is similar to the region where the enzyme can easily transform between the two conformers. It is of interest to point out that only the active transport, and not the partial reactions, exhibits maximum activity at approx. 7.5. The equilibrium-exchange reaction is almost pH independent, and the efflux of lactose exhibits a continuous decrease in the activity between pH 4 and pH 9.5 [43,44]. The downhill lactose accumulation by whole cells was reported to be practically pH independent [8]. Apparently, the transition between the two conformers is exclusive to the active transport.

The identity of the residue(s) controlling the transition has not been confirmed. The mutations described by He et al. [43] suggest that an ion pair, between residues D237 and K358, is essential for activity, but in all these cases the pH optimum was conserved. Thus, neither D237 nor K358 is involved in the reported transition. The carboxylate E325 (with $pK \approx 10$) is essential for catalysis and should be in its protonated state before the substrate can react with the enzyme [5,38]. There are two reasons to negate E325 as the residue involved in the conformation transition; the first one is its high pK, while the second is that the E325D mutant, just like the WT, exhibits maximal transport at a pH of approx. 7.5 [42]. It is of interest to point out that our analysis revealed the presence of one intracavity proton binding site with a $pK = 7.3$. It is possible that this residue, tentatively identified as H322, might have a fundamental mechanistic function.

We propose that the catalytic cycle of lac permease combines a shift of the protein between two un-isotropic configurations (periplasmic vs. cytoplasmic orientation of the open cleft) together with high and low affinity for the substrate. In one conformation, the substrate is readily accessed by water and its interaction with the protein is weak. In the other state, the substrate is stabilized by interaction with the side chains of the residues in the active site. During the substrate release step, the lactose interactions with the protein are replaced by its solvation. Our observations with the bound fluorescein could record these two states. The replacement of protein–dye interaction by water–dye interactions was detected by the protonation rate of the bound fluorescein. In the high pH regime, the fluorescein is at almost contact distance from the E126 carboxylate moiety, while the

accessibility of free protons to the dye is slower than a diffusion controlled reaction. In the other configuration, the carboxylate–chromophore interaction was canceled and the protonation of the dye is diffusion controlled. Thus, the transition from the high to the low pH regime exhibits some of the characteristics associated with the substrate expelling step of the catalytic cycle.

Finally, the same basic features, where the enzyme exhibits two conformation states that differ in the accessibility of the bound fluorescein to bulk protons with a sharp transition at the same pH range, were recorded with lipoprotein vesicles of lac permease (Nachliel and Gutman, unpublished results).

Acknowledgements

The authors are grateful to Johannes Le-Coutre (University of California, Los Angeles) for providing us with the pure preparations of the enzymes and to H. Ronald Kaback (University of California, Los Angeles) for his interest and the criticism. This research is supported by the United States–Israel Binational Science Foundation (Grant 97-130) and the German–Israeli Foundation for Scientific Research and Development (Grant I-140-207.98).

References

[1] P. Viitanen, M.J. Newman, D.L. Foster, T.H. Wilson, H.R. Kaback, Purification, reconstitution, and characterization of the lac permease of *Escherichia coli*, Methods Enzymol. 125 (1986) 429–452.

[2] S. Frillingos, M. Sahin-Tothm, J. Wu, H.R. Kaback, Cys-scanning mutagenesis: a novel approach to structure-function relationship in polytopic membrane proteins, FASEB J. 12 (1998) 1281–1299.

[3] H.R. Kaback, in: W.N. Konings, H.R. Kaback, J.S. Lolkema (Eds.), Handbook of Biological Physics: Transport Process in Eukaryotic and Prokaryotic Organisms, Elsevier, Amsterdam, 1996, pp. 203–227.

[4] H.R. Kaback, J. Voss, J. Wu, Helix packing in polytopic membrane proteins: the lactose permease of *Escherichia coli*, Curr. Opin. Struct. Biol. 7 (1997) 537–542.

[5] H.R. Kaback, J. Wu, From membrane to molecule to the third amino acid from the left with a membrane transport protein, Q. Rev. Biophys. 30 (1997) 333–364.

[6] J. Wu, D. Hardy, H.R. Kaback, Site-directed chemical cross-linking demonstrates that helix IV is close to helices VII and XI in the lactose permease, Biochemistry 38 (1999) 1715–1720.

[7] S. Frillingos, H.R. Kaback, Probing the conformation of the lactose permease of *Escherichia coli* by in situ site-directed sulfhydryl modification, Biochemistry 35 (1996) 3950–3956.

[8] J.L. Johnson, R.J. Brooker, A K319N/E325Q double mutant of the lactose permease co-transports H^+ with lactose. Implications for a proposed mechanism of H^+/lactose symport, J. Biol. Chem. 274 (1999) 4074–4081.

[9] A.E. Jessen-Marshall, N.J. Parker, R.J. Brooker, Suppressor analysis of mutations in the loop 2-3 motif of lactose permease: evidence that glycine-64 is an important residue for conformational changes, J. Bacteriol. 179 (1997) 2616–2622.

[10] J.S. Patzlaff, J.A. Moeller, B.A. Barry, R.J. Brooker, Fourier transform infrared analysis of purified lactose permease: a monodisperse lactose permease preparation is stably folded, alpha-helical, and highly accessible to deuterium exchange, Biochemistry 37 (1998) 15363–15375.

[11] C. Weitzman, H.R. Kaback, Cysteine scanning mutagenesis of helix V in the lactose permease of *Escherichia coli*, Biochemistry 34 (1995) 9374–9379.

[12] H. Jung, K. Jung, H.R. Kaback, Cysteine 148 in the lactose permease of *Escherichia coli* is a component of a substrate binding site. 1. Site-directed mutagenesis studies, Biochemistry 33 (1994) 12160–12165.

[13] J. Wu, H.R. Kaback, Cysteine 148 in the lactose permease of *Escherichia coli* is a component of a substrate binding site. 2. Site-directed fluorescence studies, Biochemistry 33 (1994) 12166–12171.

[14] S. Frillingos, J. Wu, P. Venkatesan, H.R. Kaback, Binding of ligand or monoclonal antibody 4B1 induces discrete structural changes in the lactose permease of *Escherichia coli*, Biochemistry 36 (1997) 6408–6414.

[15] M. Eigen, Proton transfer, acid-base catalysis and enzymic hydrolysis, Angew. Chem. Int. Ed. 3 (1964) 1–19.

[16] A. Weller, Excited state proton transfer, Prog. Reaction Kinetics 1 (1961) 198–214.

[17] N. Agmon, Hydrogen bonds, water rotation and proton mobility, J. Chem. Phys. 93 (1996) 1714–1736.

[18] M. Gutman, E. Nachliel, Y. Tsfadia, Propagation of protons at the water membrane interface microscopic evaluation of macroscopic process, in: E.A. Disalvo, S.A. Simon (Eds.), Permeability and Stability, CRS Press, Boca Raton, FL, 1995, pp. 259–276.

[19] M. Gutman, E. Nachliel, Time-resolved dynamics of proton transfer in proteinous systems, Annu. Rev. Phys. Chem. 48 (1997) 329–356.

[20] M. Gutman, E. Nachliel, The dynamic aspects of proton transfer processes, Biochim. Biophys. Acta 1015 (1990) 391–414.

[21] M. Gutman, D. Huppert, Rapid pH and deltamuH^+ jump by short laser pulse, J. Biochem. Biophys. Methods 1 (1979) 9–19.

[22] M. Gutman, The pH jump: probing of macromolecules and

solutions by a laser-induced, ultrashort proton pulse – theory and applications in biochemistry, Methods Biochem. Anal. 30 (1984) 1–103.

[23] E. Nachliel, M. Gutman, S. Kiryati, N.A. Dencher, Protonation dynamics of the extracellular and cytoplasmic surface of bacteriorhodopsin in the purple membrane, Proc. Natl. Acad. Sci. USA 93 (1996) 10747–10752.

[24] S. Checover, E. Nachliel, N.A. Dencher, M. Gutman, Mechanism of proton entry into the cytoplasmic section of the proton-conducting channel of bacteriorhodopsin, Biochemistry 36 (1997) 13919–13928.

[25] M. Gutman, E. Nachliel, Kinetic analysis of protonation of a specific site on a buffered surface of a macromolecular body, Biochemistry 24 (1985) 2941–2946.

[26] Y. Marantz, E. Nachliel, A. Aagaard, P. Brzezinski, M. Gutman, The proton collecting function of the inner surface of cytochrome *c* oxidase from *Rhodobacter sphaeroides*, Proc. Natl. Acad. Sci. USA 95 (1998) 8590–8595.

[27] V. Sacks, Y. Marantz, A. Aagaard, S. Checover, E. Nachliel, M. Gutman, The dynamic feature of the proton collecting antenna of a protein surface, Biochim. Biophys. Acta 1365 (1998) 232–240.

[28] Y. Marantz, E. Nachliel, Gauging of cytochrome *c* structural fluctuation by time resolved proton pulse, Isr. J. Chem. 39 (1999) 439–446.

[29] E. Pines, D. Huppert, N. Agmon, Geminate recombination in excited state proton transfer reactions, J. Chem. Phys. 88 (1988) 5620–5630.

[30] R. Yam, E. Nachliel, M. Gutman, Time-resolved proton-protein interaction. Methodology and kinetic analysis, J. Am. Chem. Soc. 110 (1988) 2636–2640.

[31] E. Nachliel, M. Gutman, Time resolved proton-phospholipid interaction. Methodology and kinetic analysis, J. Am. Chem. Soc. 110 (1988) 2629–2635.

[32] S. Checover et al., Dynamics of proton transfer reaction on the cytoplasmic surface of Bacteriorhodopsin, Biochemistry 36 (2001) 13919–13928.

[33] M. Gutman, E. Nachliel, E. Gershon, Effect of buffer on kinetics of proton equilibration with a protonable group, Biochemistry 24 (1985) 2937–2941.

[34] M. Gutman, E. Nachliel, The dynamic aspects of proton transfer processes, Biochim. Biophys. Acta 1015 (1990) 391–414.

[35] M. Gutman, E. Nachliel, The dynamics of proton exchange between bulk and surface groups, Biochim. Biophys. Acta 1231 (1995) 123–138.

[36] E. Nachliel, N. Polak, D. Huppert, M. Gutman, Time resolved study of the inner space of Lac permease, Biophys. J. 80 (2001) 1498–1506.

[37] P. Venkatesan, H.R. Kaback, The substrate-binding site in the lactose permease of *Escherichia coli*, Proc. Natl. Acad. Sci. USA 95 (1998) 9802–9807.

[38] H.R. Kaback, A molecular mechanism for energy coupling in a membrane transport protein, the lactose permease of *Escherichia coli*, Proc. Natl. Acad. Sci. USA 94 (1997) 5539–5543.

[39] M. Sahin-Toth, A. Karlin, H.R. Kaback, Unraveling the mechanism of lac permease of *E. coli*, Proc. Natl. Acad. Sci. USA 97 (2000) 10729–10732.

[40] E. McKenna, D. Hardy, H.R. Kaback, Insertional mutagenesis of hydrophilic domains in the lactose permease of *Escherichia coli*, Proc. Natl. Acad. Sci. USA 89 (1992) 11954–11958.

[41] N.J. Pazdernik, S.M. Cain, R.J. Brooker, An analysis of suppressor mutations suggests that the two halves of the lactose permease function in a symmetrical manner, J. Biol. Chem. 272 (1997) 26110–26116.

[42] S. Frillingos, H.R. Kaback, Monoclonal antibody 4B1 alters the pKa of a carboxylic acid at position 325 (helix X) of the lactose permease of *Escherichia coli*, Biochemistry 35 (1996) 10166–10171.

[43] M.M. He, J. Voss, W.L. Hubbell, H.R. Kaback, Use of designed metal-binding sites to study helix proximity in the lactose permease of *Escherichia coli*. 1. Proximity of helix VII (Asp237 and Asp240) with helices X (Lys319) and XI (Lys358), Biochemistry 34 (1995) 15661–15666.

[44] S. Frillingos, H.R. Kaback, Monoclonal antibody 4B1 alters the pKa of a carboxylic acid at position 325 (helix X) of the lactose permease of *Escherichia coli*, Biochemistry 35 (1996) 10166–10171.